

DESIGN OF QWR POWER COUPLER FOR THE RARE ISOTOPE SCIENCE PROJECT IN KOREA *

Ilkyoung Shin[†], Myung Ook Hyun, Institute for Basic Science, Daejeon, Korea
 Chang-Kyu Sung, Korea University, Sejong, Korea
 Eiji Kako, KEK, Tsukuba, Japan

Abstract

A power coupler has been designed for the Rare Isotope Science Project (RISP) in Korea. The power couplers will provide 4 kW RF power to 81.25 MHz superconducting quarter wave resonators with $\beta = 0.047$. The coupler is a coaxial capacitive type with an impedance of 50 Ω using a disc type ceramic window. Design studies of the coupler are presented.

INTRODUCTION

A heavy ion accelerator, named RAON, is under construction for the Rare Isotope Science Project (RISP) at the Institute of Basic Science (IBS) in Korea [1]. A driver linac utilizes Quarter Wave Resonators (QWRs) and Half Wave Resonators (HWRs) to accelerate ions to 18.5 MeV/u. A power coupler for QWR has been designed to deliver 4 kW RF power at 81.25 MHz in CW mode. The coupler is designed to handle a full reflected power at the maximum incident power. Table 1 shows coupler design parameters.

Table 1: Coupler Design Parameters

Parameter	Value
Frequency	81.25 MHz
Operational power	4 kW
S_{11} at 81.25 MHz	< 30 dB
Impedance	50 Ω
Q_{ext}	2×10^6
Coupling type	fixed

COUPLER STRUCTURE

Figure 1 shows the coupler structure. The coaxial structure is based on 50 Ω coaxial line. The coupler has a disc type ceramic window. The structure around the ceramic window is optimized to minimize a reflected RF power and to accommodate three ports for diagnostics. Three diagnostic devices are a vacuum gauge, an e-pickup, and an arc detector. One thermal intercept is located at 40 K. A bellow structure compensates for thermal contraction and gives a flexibility in assembly with a cryomodule. The outer conductor is made of a stainless steel with 20 μm copper plating on

the inside surface. The hollow inner conductor is made of OHFC copper.



Figure 1: QWR RF power coupler. Coaxial capacitive structure with 50 Ω using a disc type ceramic window.

SIMULATIONS

Electromagnetic, thermal, and mechanical simulations were performed using the CST and ANSYS simulation packages.

Electromagnetic Simulation

CST Microwave Studio and HFSS were used to analyze and optimize RF properties of the coupler. The EM simulation results were sent to CST MPhysics and ANSYS Thermal solver for thermal analysis. Figure 2 shows an EM simulation model for CST Microwave Studio.

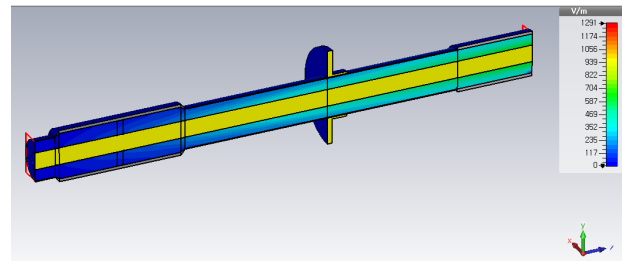


Figure 2: EM simulation model. Electric field distribution.

The location of the power and pickup couplers were simulated using CST Microwave Studio eigen mode solver. The antenna tip of the power coupler is located at 15 mm into the cavity for $Q_{ext} = 2 \times 10^6$. The Q_{ext} of the pickup coupler is 1×10^{11} , and the tip is placed at 35 mm out of cavity. Figure 3 shows the locations of the power and pickup couplers.

* This work was supported by the Rare Isotope Science Project of Institute for Basic Science funded by the Ministry of Science, ICT and Future Planning (MSIP) and the National Research Foundation (NRF) of the Republic of Korea under Contract 2013M7A1A1075764.

[†] ishin@ibs.re.kr

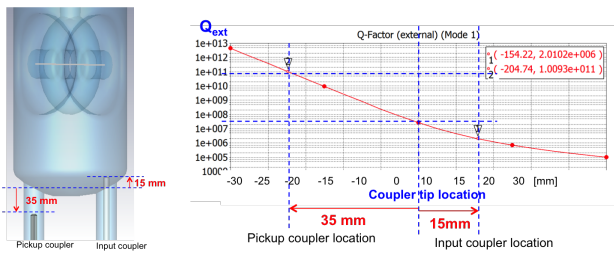


Figure 3: Locations of power and pickup couplers. Power coupler at 15 mm into cavity and pickup coupler at 35 mm out of cavity.

Multipacting Simulation

Multipacting simulation was performed using CST Particle Studio. The simulation results show that mutipacting occurs at RF power lower than about 300 W for 50 Ω coaxial structure of the coupler. The impedance around the ceramic window is 58 Ω and multipacting occurred at RF power lower than about 800 W. These results are well agree with the scaling law of mutipacting in coaxial lines [2]. The multipacting band is much lower than the nominal operation power of 4 kW. Figure 4 shows multipacting simulation results for two different coaxial structures.

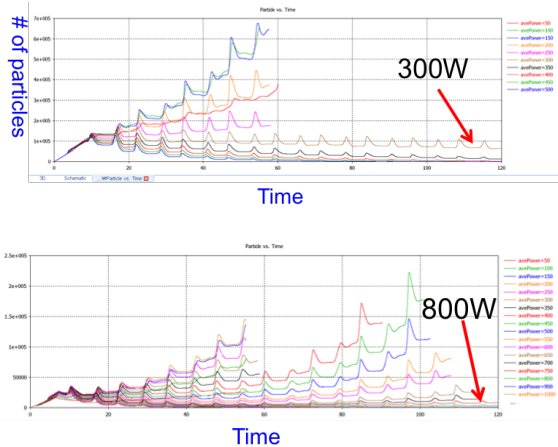


Figure 4: Multipacting analyses for 50 Ω (top) and 58 Ω coaxial lines (bottom).

Thermal Simulation

The thermal analysis were performed with CST MPhysics and ANSYS Thermal solver. In CST simulation, the tetrahedral mesh instead of the hexahedral mesh was applied for the thermal analysis because the hexahedral mesh is not suitable for a thin copper plating structure [3]. Temperature dependent properties such as thermal conductivity, electric conductivity, and heat capacity, are modeled by dividing the CST model into pieces [4].

The dissipated RF power used in thermal simulation was obtained from CST Microwave Studio and HFSS, and then they were coupled to CST Physics and ANSYS Thermal solver. Figure 5 shows a a temperature distribution with

4 kW RF power. Temperatures at antenna tip and ceramic window are shown in Table 2 for three RF powers. A cross-check of the thermal analyses with CST and ANSYS will be performed and actual temperature will be measured for prototype couplers to confirm the necessity of an active cooling scheme. Static thermal loads are 0.6 W and 7.4 W at 4.5 K and 40 K thermal intercepts, respectively.

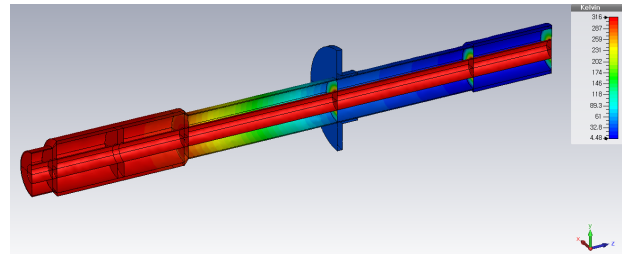


Figure 5: Temperature distribution. Thermal intercepts are located at 40 K and the cavity is at 4.5 K.

Table 2: Temperature at Antenna Tip and Ceramic Window

RF power	Antenna tip	Ceramic window
0 kW	293 K	297 K
4 kW	311 K	309 K
16 kW	361 K	341 K

Mechanical Simulation

CST MPhysics and ANSYS Structural, Modal, and Harmonic Response were used for mechanical analysis.

- Stress on ceramic window

Mechanical analysis due to gravity indicates that the stress on the ceramic window is two orders of magnitude smaller than the maximum flexural stress. The inner conductor made of OFHC copper is in a linear elastic regime in stress-strain curve [5]. Figure 6 shows stress and strain analyses due to gravity around the ceramic window.

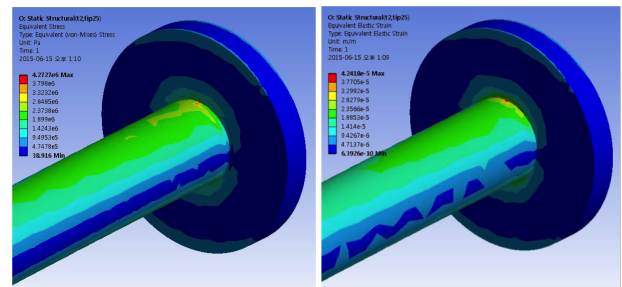


Figure 6: Stress and strain due to gravity around ceramic window.

- Modal analysis

The modal analysis was performed using ANSYS Modal solver to identify the vibrational mode of the

inner conductor. Efforts were made to avoid a modal frequency of 60 Hz, which is an AC electric power frequency. Figure 7 shows first four vibrational modes.

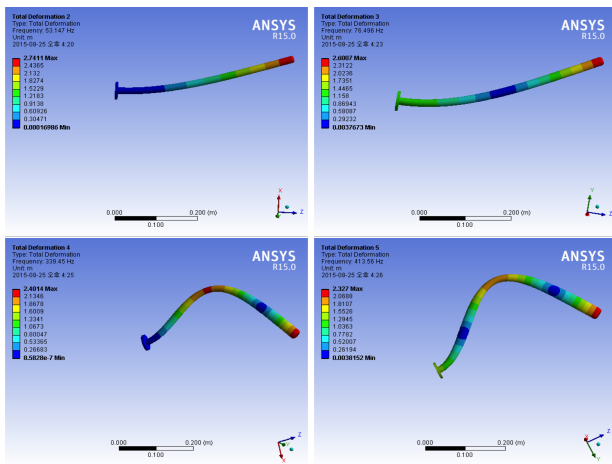


Figure 7: Four vibrational modes of inner conductor.

The modal frequencies of the inner conductor are listed in Table 3. A harmonic response study shows that both of the mode 1 and 2 are sensitive to vibration and they should be carefully considered in design stage to avoid 60 Hz.

Table 3: Vibrational Mode of Inner Conductor

Mode	Frequency
Mode 1	53.1 Hz
Mode 2	76.5 Hz
Mode 3	339.5 Hz
Mode 4	413.6 Hz

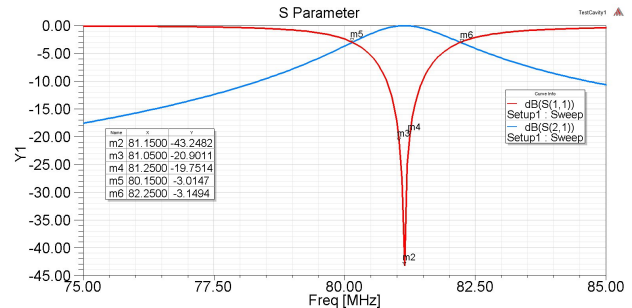
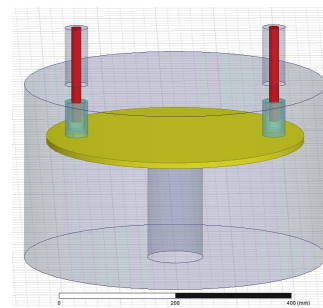


Figure 8: Test chamber for RF conditioning and S parameter.

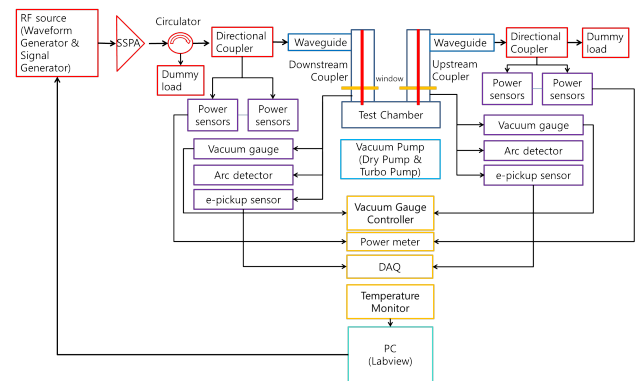


Figure 9: Schematic of RF conditioning system.

RF CONDITIONING SYSTEM

Test Chamber

A test chamber for RF conditioning is in design stage. The structure benchmarked the test chamber for the IFMIF coupler and the cADS coupler [6, 7]. The pass band around 81.25 MHz is narrow (about 0.2 MHz for $S_{11} < -20$ dB). A tuner from the top plate will be installed to adjust the frequency. Figure 8 shows an EM design model and its S parameters.

Monitoring and Interlock System

Vacuum gauges, temperature sensors, arc detectors, e-pickups will be installed for diagnostic purpose during RF conditioning. A control system using Labview software is being developed to monitor and archive data from diagnostic devices and to protect RF and vacuum systems using vacuum, temperature, and arc signals. Figure 9 and 10 shows a schematic diagram of RF conditioning system and its user interface.

FUTURE PLAN

The prototype of the coupler and the test chamber will be manufactured, and RF conditioning will be performed using a monitoring and interlock system. The simulation results and measurements during RF conditioning will be compared.

ACKNOWLEDGMENT

The authors would like to thank the cryomodule colleagues; Youngkwon Kim, Minki Lee, Yong Woo Jo, Jong Wan Choi, Woo Kang Kim, for their support and discussions to establish the coupler assembly with a cryomodule.

Special thanks should go to Jeongseog Song for many helps in Labview system development.

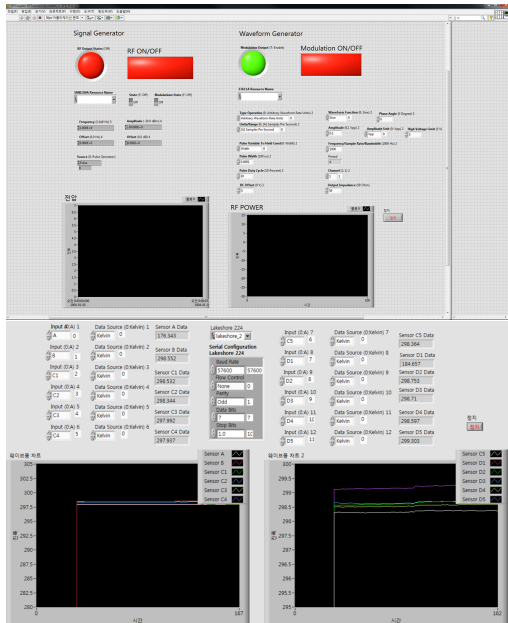


Figure 10: Control system interface.

REFERENCES

- [1] D. Jeon et al, “Design of the RAON Accelerator Systems”, J. Korean Phys. Soc. 65, issue 7, 1010 (2014).
- [2] E. Somersalo et. al., “Analysis of Multipacting in Coaxial Lines”, Proc. of the Particle Accelerator Conference (1995).
- [3] S. V. Kutsaev, M. P. Kelly and P. N. Ostroumov Design of RF power coupler for superconducting cavities, Journal of Instrumentation, Volume 7, November 2012
- [4] M.P. Kelly et al., “DESIGN AND CONSTRUCTION OF A HIGH-POWER RF COUPLER FOR PXIE”, Proc. of the IPAC2012, New Orleans, Louisiana (2012)
- [5] D. Rittel et. al., “Large strain constitutive behavior of OFHC copper over a wide range of strain rates using the shear compression specimen”, Mechanics of Materials 34 (2002) 627-642
- [6] D. Regidor et. al., “IFMIF-EVEDA SRF LINAC COUPLERS TEST BENCH”, Proc. of the IPAC2013, Shanghai (2013)
- [7] Chen Xu et. al., “Coupler conditioning and high power testing of ADS Spoke cavity”, Chinese Physics C, Volume 38, Number 2 (2014)